PNAS
www.pnas.org

Supplementary Information for
Synaptic plasticity rules with physiological calcium levels

Yanis Inglebert[1,*], Johnatan Aljadeff[2,3,*], Nicolas Brunel[2,3], Dominique Debanne[1]

1 UNIS, INSERM Aix-Marseille Université, Marseille France
2 University of Chicago, USA
3 Duke University, USA
* These authors contributed equally to the work

Correspondence:
dominique.debanne@univ-amu.fr (DD), nicolas.brunel@duke.edu (NB)

This pdf includes:

- Supplementary text
- Figures S1 to S7
- Tables S1 to S4
- Supplementary references

Supplementary text

1 Synaptic plasticity model

1.1 Calcium transients

Calcium transients in the model depend on the pre- and post-synaptic spiking activity, and indirectly on the extracellular calcium concentration (through scaling of the amplitude parameters with $[Ca^{2+}]$). The pre- and post-synaptic spike trains are denoted by $s_{\rm pre} = \sum_i \delta(t - t_{i,\rm pre})$ and $s_{\rm post} = \sum_i \delta(t - t_{i,\rm post})$, respectively. The temporal evolution of the pre- and post-synaptically induced calcium transients is given by:

$$\frac{d}{dt}c_{\rm pre}(t) = -\frac{1}{\tau_{\rm Ca}}c_{\rm pre}(t) + C_{\rm pre}s_{\rm pre}(t-D) \quad (1)$$

$$\frac{d}{dt}c_{\rm post}(t) = -\frac{1}{\tau_{\rm Ca}}c_{\rm post}(t) + C_{\rm post}s_{\rm post}(t) \quad (2)$$

where $C_{\rm pre}$ and $C_{\rm post}$ are parameters describing the magnitude of jumps in calcium following a pre- and a post-synaptic spike, D is a pre-synaptic delay parameter and $\tau_{\rm Ca}$ is the decay timescale of calcium transients.

The equation for the time evolution of the nonlinear contribution $c_{\rm NL}(t)$ is

$$\frac{d}{dt}c_{\rm NL}(t) = -\tau_{\rm Ca,NMDA}c_{\rm NL}(t) + \eta c_{\rm pre}(t)c_{\rm post}(t) \quad (3)$$

where $\tau_{\rm Ca,NMDA}$ is the decay timescale of the nonlinear transients and η is a parameter describing the strength of the nonlinearity. The total transient $c(t)$ is then

$$c(t) = c_{\rm pre}(t) + c_{\rm post}(t) + c_{\rm NL}(t), \quad (4)$$

The amplitude parameters $C_{\rm pre}$, $C_{\rm post}$ depend on the extracellular calcium concentration through the scaling exponents $a_{\rm pre}$, $a_{\rm post}$:

$$\frac{C_{\rm pre}([Ca^{2+}]_1)}{C_{\rm pre}([Ca^{2+}]_2)} = \left(\frac{[Ca^{2+}]_1}{[Ca^{2+}]_2}\right)^{a_{\rm pre}} \quad (5)$$

$$\frac{C_{\rm post}([Ca^{2+}]_1)}{C_{\rm post}([Ca^{2+}]_2)} = \left(\frac{[Ca^{2+}]_1}{[Ca^{2+}]_2}\right)^{a_{\rm post}} \quad (6)$$

In addition to the full nonlinear model described by the equations above, we considered linear models where the calcium transient is a sum over pre- and post-synaptic contributions only, i.e., $c(t) = c_{\rm pre}(t) + c_{\rm post}(t)$ (equivalently, one can set $\eta = 0$).

We also considered a model in which there is no linear post-synaptic contribution. The equations for the time evolution of calcium transients in that case are the same as above, with $c(t) = c_{\rm pre}(t) + c_{\rm NL}(t)$ (note that the post-synaptic transient must still be computed to then compute the nonlinear one).

1.2 Synaptic weight dynamics

In our model, synaptic weight dynamics are graded, i.e., any synaptic weight value between $w_{\min}$ and $w_{\max}$ is stable if there is no crossing of the depression (and potentiation) threshold. The weight variable w is restricted to this range using soft thresholds, so the equation for the time evolution of w is

$$\frac{d}{dt}w(t) = \gamma_p(w_{\max} - w(t))\Theta\left[c(t) - \theta_p\right] - \gamma_d(w - w_{\min})\Theta\left[c(t) - \theta_d\right]. \tag{7}$$

Here, Θ is the heaviside step function; γ_p and γ_d are the potentiation and depression rates, respectively; and θ_p and θ_d are the potentiation and depression thresholds above which the synaptic weight variable increases or decreases.

2 Fitting model to data

We fit the calcium based plasticity model to the experimental STDP curves at three calcium concentrations using the procedure described below. The central part of the fitting procedure is to mathematically express the relative change in synaptic efficacy Δw as a function of the induction protocol, the extra-cellular calcium concentration $[Ca^{2+}]$ and the model parameters.

The function Δw is computed in two steps as a function of these variables. First we compute the time the intra-cellular calcium variable $c(t)$ spends above the depression and potentiation thresholds: T_d and T_p, respectively. In the second step we use T_d, T_p and the rest of the variables and parameters to compute Δw.

Computation of calcium transients and time spent above threshold

For induction protocols with low pairing frequencies one can assume that the transient calcium returns to baseline before each repetition. This assumption holds for a paring frequency of 0.3Hz used for most of our measurements (and *all* the data used for model fitting purposes), making it sufficient to compute transients for a single repetition of each protocol. Furthermore, when a protocol consists of a single pre- and a single post-synaptic spike occurring at $t = 0$, $t = \Delta t$, respectively, Eqs. (1-3) can be solved analytically:

$$c_{\text{pre}}(t) = \Theta(t - D)C_{\text{pre}} \exp\left(-\frac{t - D}{\tau_{\text{Ca}}}\right) \tag{8}$$

$$c_{\text{post}}(t) = \Theta(t - \Delta t)C_{\text{pre}} \exp\left(-\frac{t - \Delta t}{\tau_{\text{Ca}}}\right) \tag{9}$$

$$\begin{aligned} c_{\text{NL}}(t) = {} & \frac{\Theta\left[t - \max(D, \Delta t)\right]}{\frac{2}{\tau_{\text{Ca}}} - \frac{1}{\tau_{\text{Ca,NMDA}}}} \eta C_{\text{pre}} C_{\text{post}} \exp\left(\frac{D + \Delta t}{\tau_{\text{Ca}}}\right) \\ & \times \left[\exp\left(\max(D, \Delta t)\left(\frac{1}{\tau_{\text{Ca,NMDA}}} - \frac{2}{\tau_{\text{Ca}}}\right)\right) e^{-\frac{t}{\tau_{\text{Ca,NMDA}}}} - e^{-\frac{t}{\tau_{\text{Ca}}/2}}\right]. \end{aligned} \tag{10}$$

The calcium transient was computed using these expressions and Eq. (4) with temporal resolution $dt = 0.25$ ms.

For protocols with a post-synaptic burst of spikes, $c_{\rm post}$ and $c_{\rm NL}$ were computed by replacing Δt in Eqs (9,10) with the times of the spikes in the post-synaptic burst (relative to the pre-synaptic spike at $t = 0$) and summing over all the spikes in the burst of the post-synaptic neuron[1]. When the pairing frequency is low, the calcium variable $c(t)$ returns to baseline between repeated stimulation. Therefore, for low pairing frequencies (below 1Hz), for both single spikes and bursts,$c(t)$ is computed analytically for one repeat of the protocol [using Eqs. (8-10)]. The result of that calculation is then used to compute the predicted change in synaptic weight (see below).

For protocols with high pairing frequency where the calcium transient does not necessarily return to baseline following each repeat of the induction protocol, the transients were computed using the Euler method with time-step $dt = 0.25$ms. Using a smaller time-steps made fitting considerably slower but it did not change the results.

The time spent above the depression and potentiation thresholds (during each repeat of the induction protocol of duration T) is then

$$T_d = \int_0^T \Theta(c(t) - \theta_d)dt \tag{11}$$

$$T_p = \int_0^T \Theta(c(t) - \theta_p)dt. \tag{12}$$

The integrals were approximated by counting temporal bins in which $c(t)$ exceeded the threshold and multiplying by dt. Note that for the linear model ($\eta = 0$), T_d and T_p can be computed analytically (see [1]).

Computation of Δw

The synaptic weight variable evolves according to Eq. (7). We assume that changes to synaptic weights are slow relative to the pairing frequency, allowing us to average the weight change due to one repeat of the protocol [RHS of Eq. (7)]. From this, one can show that if the initial value $w(t = 0) = 1$ and the protocol is repeated n times, the synaptic weight variable at the end of the protocol $w_f = w(t = nT)$ is

$$w_f = \bar{w} + (1 - \bar{w}) \exp(-n/\tau_{\rm eff}), \tag{13}$$

where

$$\bar{w} = \frac{\gamma_p T_p w_{\max} + \gamma_d T_d w_{\min}}{\gamma_p T_p + \gamma_d T_d} \tag{14}$$

$$\tau_{\rm eff} = \frac{T}{\gamma_p T_p + \gamma_d T_d}. \tag{15}$$

Note that if the synaptic weight saturates to $\bar{w}$ (i.e., $\exp(-n/\tau_{\rm eff}) \approx 0$), the predicted plasticity is invariant under rescaling of γ_d, γ_p.

By assumption the synaptic weight at time 0 is $w(t) = 1$, so the relative change in synaptic efficacy as a function of the protocol and the model parameters is simply

$$\Delta w = w_f. \tag{16}$$

[1] This is only valid because there was a single pre-synaptic stimulation in every repetition of the induction protocol. Had there been more than a single pre-synaptic stimulation then computing $c_{\rm NL}$ requires solving Eqs. (8-10) explicitly.

3 Using the imaging experiments to constrain model parameters

In the imaging experiments, we measured the calcium fluorescence in postsynaptic spine under different stimulation protocols and in preparations with differing calcium concentrations. We used the results of these experiments to constrain the parameters of the calcium based plasticity model. Specifically, we computed the area under the $\Delta G/F$ curve of resulting from protocols with one pre- and 1, 2, 3 or 4 post-synaptic spikes (Figures 3, 4), measured at different extracellular calcium concentrations. This is thought to be proportional to the total calcium entry following a given stimulus at a given concentration. The quantity that was related to data was then the ratio of total calcium entry for a two post-synaptic spike stimulus relative to a protocol with a single post-synaptic spike (denoted r_2). At $[Ca^{2+}] = 1.3$ mM we have $r_2 = 1.05 \pm 0.26$, while at $[Ca^{2+}] = 3$ mM we have $r_2 = 1.88 \pm 0.42$ (mean $\pm$ standard deviation). We also considered measurements of calcium transients following pre-posts pairs of spikes with positive and negative timing ($\Delta t = \pm 20$ ms). Specifically, we computed the ratio $r_\pm$ of the corresponding $\Delta G/F$ curves and found $r_\pm = 1.51 \pm 0.63$ for $[Ca^{2+}] = 1.3$ mM and 1.88 ± 0.43 for $[Ca^{2+}] = 3$ mM.

Linear case

When calcium transients are linear in the pre- and post-synaptic activity, the model parameters can be constrained to reproduce the values of r_2 measured in the experiment. These constraints are: $C_{\text{post}}/C_{\text{pre}} = 0.011$ and $a_{\text{post}} - a_{\text{pre}} = 5.93$. Assuming a_{post} and a_{pre} are non-negative (i.e., calcium amplitudes do not decrease with the extracellular concentration) implies $a_{\text{post}} \geq 5.93$. We think that such a scaling exponent is not biophysically realistic, so we interpret the imaging experiments as additional evidence that nonlinear calcium transients must be taken into account in the plasticity model.

Derivation. Let I_1 be the total calcium entry resulting from a single pre- and a single postsynaptic spike. We have,

$$I_1 = C_{\text{pre}} \rho^{a_{\text{pre}}} \tau_{\text{Ca}} \left(1 + \bar{C} \rho^{\Delta a}\right) \tag{17}$$

where ρ is the extracellular calcium concentration, and $\Delta a = a_{\text{post}} - a_{\text{pre}}$, $\bar{C} = C_{\text{post}}/C_{\text{pre}}$.
Similarly, let I_2 be the total calcium entry resulting from a single pre- and two postsynaptic spikes. Now we have,

$$I_2 = C_{\text{pre}} \rho^{a_{\text{pre}}} \tau_{\text{Ca}} \left(1 + 2\bar{C} \rho^{\Delta a}\right). \tag{18}$$

Define $r_2(\rho)$ to be the ratio of total calcium entry,

$$r_2(\rho) = \frac{I_2}{I_1} = \frac{1 + 2\bar{C}\rho^{\Delta a}}{1 + \bar{C}\rho^{\Delta a}}, \tag{19}$$

so,

$$\Delta a = \frac{\log\left[\frac{r_2-1}{\bar{C}(2-r_2)}\right]}{\log\rho}, \tag{20}$$

$$\log\bar{C} = \frac{\frac{\log\left[\frac{r_2(1.3\text{mM})-1}{2-r_2(1.3\text{mM})}\right]}{\log 1.3} - \frac{\log\left[\frac{r_2(3\text{mM})-1}{2-r_2(3\text{mM})}\right]}{\log 3}}{\frac{1}{\log 1.3} - \frac{1}{\log 3}}. \tag{21}$$

From the experimental data we have

$$\begin{aligned} r_2\left(1.3\text{mM}\right) &= 1.048 \\ r_2\left(3.0\text{mM}\right) &= 1.876. \end{aligned} \tag{22}$$

giving

$$\begin{aligned} \bar{C} &= 0.011 \\ \Delta a &= 5.93. \end{aligned} \tag{23}$$

Nonlinear case

We expressed r_2 using the parameters of the nonlinear model, and fit model parameters subject to inequalities guaranteeing that the model's r_2 is within one or two standard deviations of its mean, computed from the experimental results. The model fits, predictions and errors are shown in **Figure 8** and **Figures S5**, **S6**.

Derivation. To express r_2 as a function of the full model parameters (including the nonlinearity), we compute the integral over the pre, postsynaptic and nonlinear terms [Eqs. (8-10)]. Restoring the explicit dependence on the calcium concentration ρ,

$$\int_{-\infty}^{\infty} c_{\text{pre}}\left(t\right) dt = C_{\text{pre}}\rho^{a_{\text{pre}}}\tau_{\text{Ca}} \tag{24}$$

$$\int_{-\infty}^{\infty} c_{\text{post}}\left(t\right) dt = C_{\text{post}}\rho^{a_{\text{post}}}\tau_{\text{Ca}} \tag{25}$$

$$\int_{-\infty}^{\infty} c_{\text{NL}}\left(t\right) dt = \frac{1}{2}\tau_{\text{Ca}}\tau_{\text{Ca,NMDA}}\eta C_{\text{pre}}C_{\text{post}}\rho^{a_{\text{pre}}+a_{\text{post}}}\exp\left(\frac{D-\Delta t}{\tau_{\text{Ca}}}\right). \tag{26}$$

Using these and the experimentally measured values of r_2 we added inequalities as constraints to our numerical optimization procedure. Specifically, the model values of r_2 were required to be within either 1 or 2 standard deviations of the empirical measurement.

4 Constraints on parameters from qualitative features of the model and the STDP curve

The constraints we used for the transient amplitude parameters C_{pre} and C_{post} ensure that a single spike by a pre- or post-synaptic neuron cannot lead to a calcium transient that exceeds

the depression threshold at the highest calcium concentration we used in our experiments ($[Ca^{2+}]$ = 3.0 mM). This constraint can be relaxed if the model is fitted to data with a single calcium concentration. One can then ensure that a pair of well separated pre- and post-synaptic spikes do not lead to changes in the synapse by requiring that the product of the time spent above threshold (T_p, T_d) and the corresponding rate (γ_p, γ_d) are equal. If transients induced by single spikes can cross threshold, this requires tuning either γ_p or γ_d such that indeed $\gamma_d T_d = \gamma_p T_p$ [1].

This scheme cannot be used when one is interested in fitting the model for multiple extracellular calcium concentrations. The reason is that if one fixes, say, γ_d such that potentiation and depression balance each other for a pair of spikes at one concentration, the same value will lead to imbalance at a different concentration.

We assumed that the calcium transients following a single pre- and post-synaptic spike decay on the same timescale, τ_{Ca}, while the time-scale associated with the nonlinear term, $\tau_{\mathrm{Ca,NMDA}}$, is longer. This assumption can be justified, at least qualitatively, by inspection of the STDP curve we measured at $[Ca^{2+}]$ = 3.0 mM and the fact that increasing the pairing-frequency above a few Hz leads to strong changes in the resulting plasticity.

From the shape of Δw as a function of Δt at high concentration we conclude that the calcium transients in the model must carry information about the relative timing of pre- and post-synaptic spikes at a resolution of approximately 20 ms. In other words, the fact that changing the relative timing of a pair of spikes by 20 ms leads to significant changes to the resulting plasticity implies that the calcium transients in the model must preserve the timing information on that timescale.

On the other hand, the impact that increasing the pairing-frequency has on the resulting plasticity implies that the model must consist of at least one transient that decays on a timescale significantly longer than 20 ms.

We further inspect the shape of the STDP curve measured at $[Ca^{2+}]$ = 3.0 mM. Especially noteworthy is the second LTD window at positive Δt. The width of that window is comparable with the first LTD window at negative Δt. Moreover, consider reflecting the data about a vertical axis at the center of the LTP window, $\Delta t \sim 20$ ms. The resulting data points give an STDP curve that overlaps the original curve, suggesting a degree of symmetry played by the pre-synaptic neuron (including the delay D) and the post-synaptic neuron. This symmetry (which is also respected by the STDP curves measured at $[Ca^{2+}]$ = 1.3, 1.8 mM) implies that one cannot associate the pre-synaptic transients with a decay timescale much shorter than that of post-synaptic transients, or vice versa.

Therefore, assuming there are no intermediate timescales between τ_{Ca} and $\tau_{\mathrm{Ca,NMDA}}$ that need to be explicitly introduced to the model, the only way to associate the timescales with transients that respects this symmetry is to let the pre- and post-synaptic transients decay with timescale τ_{Ca}, and let the nonlinear transient decay with timescale $\tau_{\mathrm{Ca,NMDA}}$. We note that this qualitative argument yields a model that is in good agreement with our measurements using plasticity using patch-clamp electrophysiology and calcium imaging. Mapping the component of the phenomenological model we present here to the details of the biophysics of calcium entry, where non-additive contributions to transients may depend asymmetrically on relative timing of pre- and post-synaptic activity, remains a question for future research.

5 Numerical optimization

Table 3 includes the range of values within which we optimized the model parameters, and the values we used (for parameters that were fixed).

The fitting error is defined to be RMS error over the 144 data points (black crosses in **Figure 8A**). The fitting error is highly nonlinear in terms of the model parameters, and therefore we cannot expect it to be convex. Hence, for each model we initialized a gradient descent routine at 2000 points chosen uniformly at random within the allowed parameter hypercube. We used the nonlinear constrained optimization built-in to the Matlab software, choosing the active-set algorithm. Using a different optimization algorithm (interior-point) had impact on the time it took to find (local) minima and the fraction of initial conditions of the parameter set that "exit" the allowed hypercube, due to the differences in how step sizes are computed in different algorithms. However, parameter sets with small fitting error given by the active-set and interior-point algorithms were close to one another in the values of the parameters, had similar fitting error (for spike-pairs) and prediction error (for bursts).

6 Parameter variation

To study the effect of varying model parameters in the neighborhood of the best fitting parameter set we multiplied each model parameter by a factor $1+0.1x$, where x is drawn at random (independently for each parameter and each repetition of this procedure) from a standard normal distribution. With these randomized parameter sets in hand, we computed the STDP curves and the changes in synaptic efficacies following all experimental protocols. These were then used to compute the error bars and shaded areas around the curves showing Δw as a function of Δt and Δw as a function of the pairing-frequency f.

7 Eliminating the linear postsynaptic contribution.

Previously published results have indicated that repeated post-synaptic stimulation, even at high frequencies, does not lead to long-term synaptic plasticity if the pre-synaptic neuron does not fire [2, 3]. Qualitatively, the model described above is inconsistent with this observation, since the post-synaptically induced calcium transient alone will summate and cross the LTD/LTP threshold for high enough frequency. We therefore asked whether our model can be modified such that it will predict no change in the synaptic efficacy for protocols where only the post-synaptic neuron is stimulated. Indeed, we find that, since the main contribution to calcium transients is nonlinear (**Figure 7**), simply dropping the post-synaptic only contribution to the total calcium transient leads to negligible changes to the model predictions for the plasticity experiments (compare **Figure 8** with **Figure S7**). Note that the post-synaptic component of the transient is still used for the purposes of computing the nonlinear contribution. We focus our discussion on the "full" model (that includes linear dependence on post-synaptic activity), but we emphasize that the data can be fit equally well with a model with such linear dependence.

Supplementary Figures

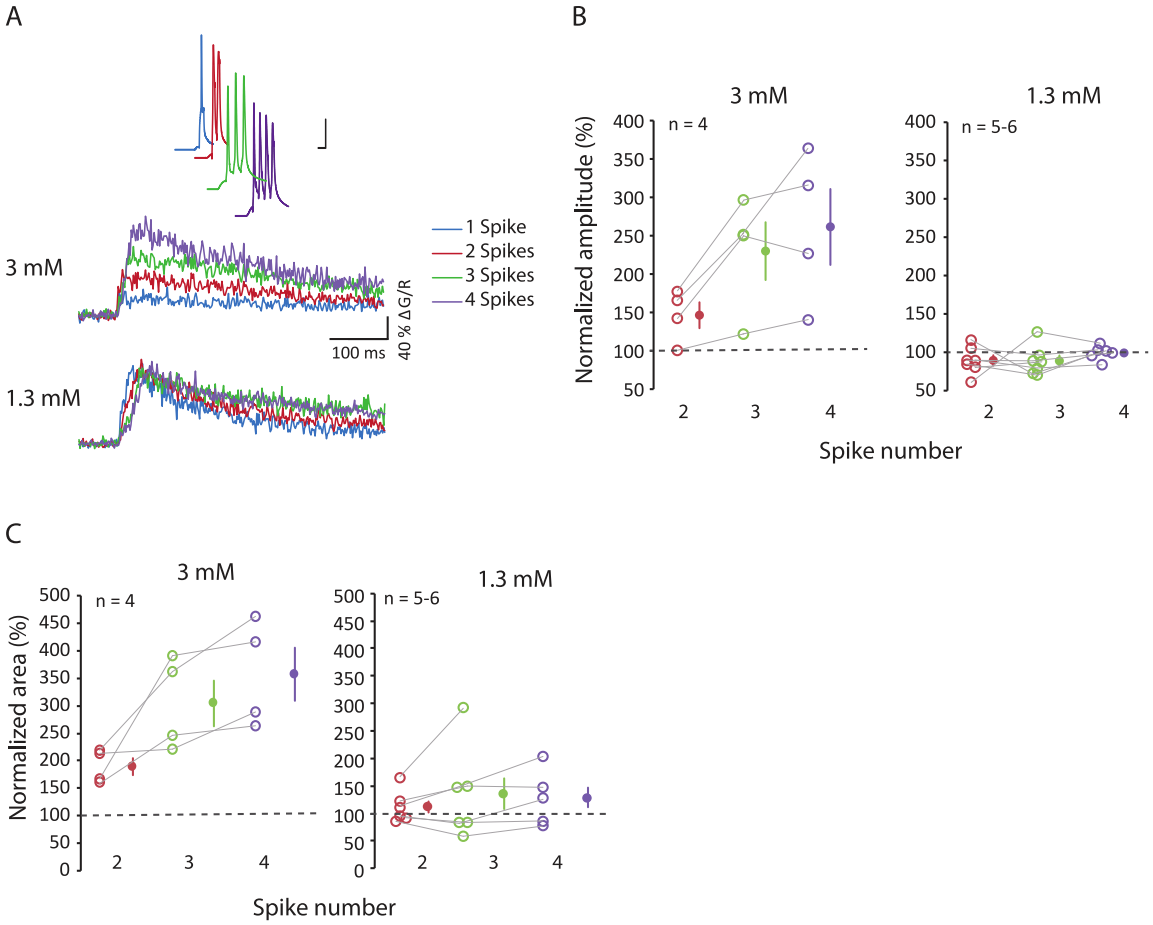

Figure S1: **Comparison of calcium transients during pre-post pairings induced with 1-4 action potentials.** (**A**) Representative traces of calcium signals measured in a single dendritic spine evoked by a pre-post protocol at $\Delta t = +20$ ms with one (blue traces), two (red traces), three (green traces) or four (purple traces) action potentials. (**B** & **C**). An almost linear summation for amplitude (**B**) and integral (**C**) is observed in 3 mM extracellular calcium but not in 1.3 mM extracellular calcium.

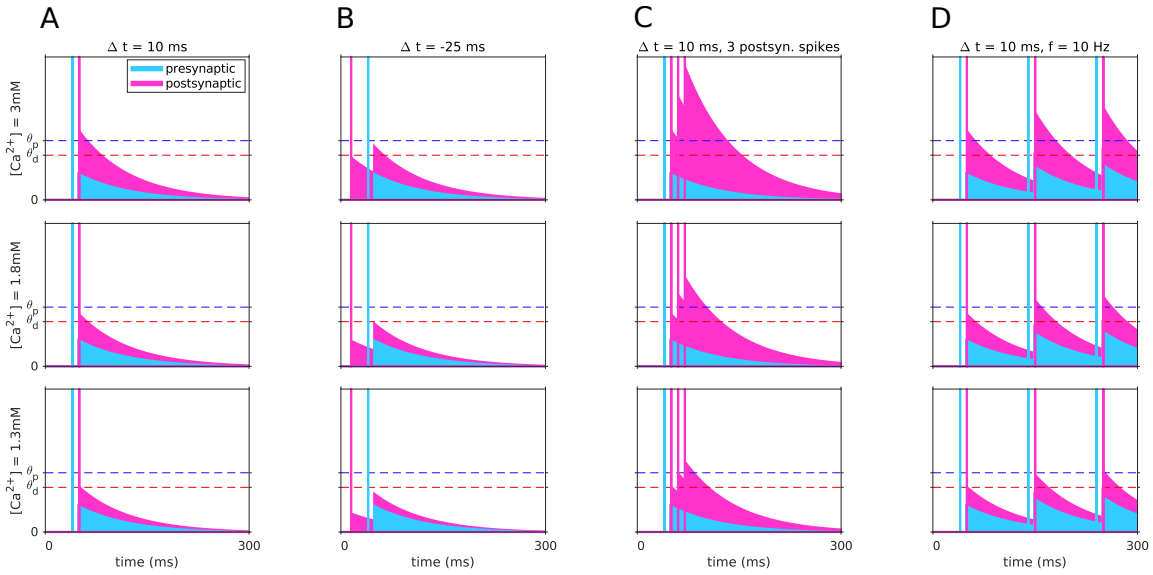

Figure S2: **Dependence of calcium transients of a linear plasticity model on the stimulation protocol and on the extracellular calcium concentration.** Same as **Figure 7**, for a model with calcium transients that are linearly dependent on pre- and post-synaptic activity. A single pre-post pairing at $\Delta t = 10$ ms (**A**), $\Delta t = -25$ ms (**B**), a pre-synaptic spike paired with a burst of three post-synaptic spikes (**C**) and a pre-post pair repeated at a frequency of 10 Hz (**D**). Transients for all stimulation protocols are shown for the three extracellular calcium concentrations used in the experiment (rows). Transients resulting from different protocols qualitatively match the observed plasticity for the same protocol in the experiment, but our analysis shows that this model does not give a good quantitative fit to the data at different concentrations and stimulation protocols.

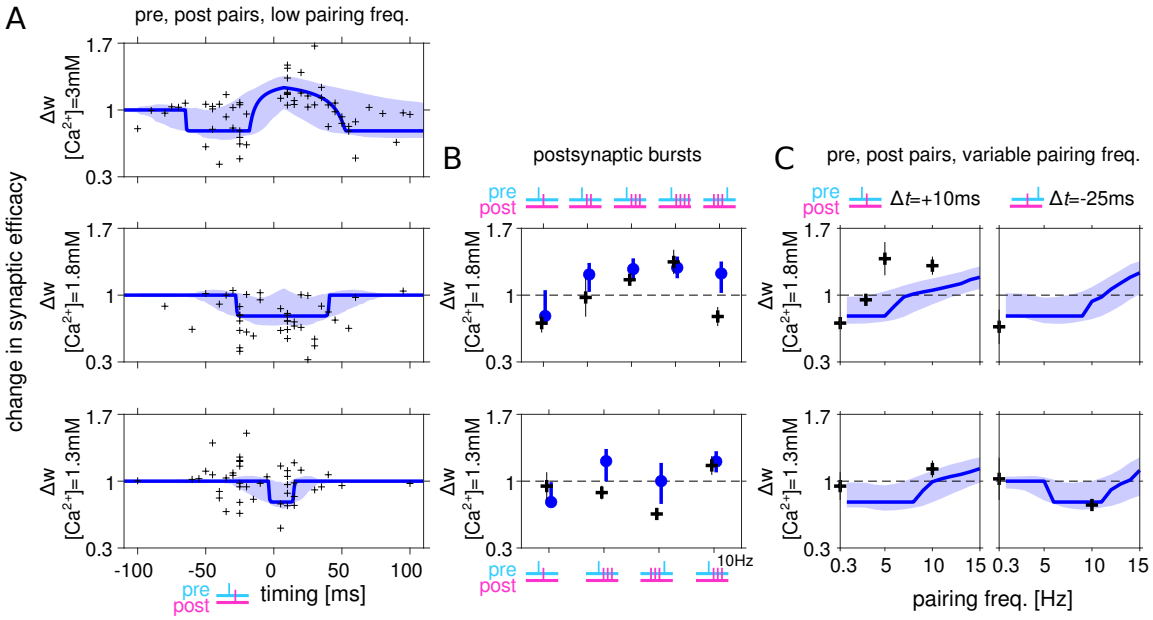

Figure S3: **A linear calcium based plasticity model fails to quantitatively account for the plasticity data at multiple concentrations.** Same as **Figure 8**, for a model with calcium transients that are linearly dependent on pre- and post-synaptic activity. (**A**) Model fit to the STDP data at $[Ca^{2+}] = 3$, 1.8, 1.3 mM. Each measured synapse is represented by a black cross. Shaded area indicates the standard deviation around the mean obtained by generating predictions using parameter sets in the neighborhood of the best fitting model. At small Δt the model correctly captures the change of sign of plasticity as the extracellular calcium concentration changes. However, the inferred decay timescale of calcium transients is long, so this model predicts significant changes to the synaptic weight even when pre- and post-synaptic spikes are separated by more than 100 ms. (**B**) Experimental results and model predictions for protocols with post-synaptic burst stimuli. At $[Ca^{2+}] = 1.8$ mM (top), the model fails to captures the change in sign of plasticity as a function of the order of a single pre- and three post-synaptic spikes. At $[Ca^{2+}] = 1.3$ mM (bottom), the model incorrectly predicts potentiation or no-change for two protocols with three post-synaptic spikes, for which LTD was measured experimentally. These inconsistencies between the model and the data are due to the long decay timescale of calcium transients, leading to saturation to LTP as a function of the number of post-synaptic spikes. (**C**) Experimental results and model predictions for protocols at variable pairing frequencies. The linear model fails to predict the pairing frequency at which the polarity of plasticity changes at $[Ca^{2+}] = 1.8$ mM.

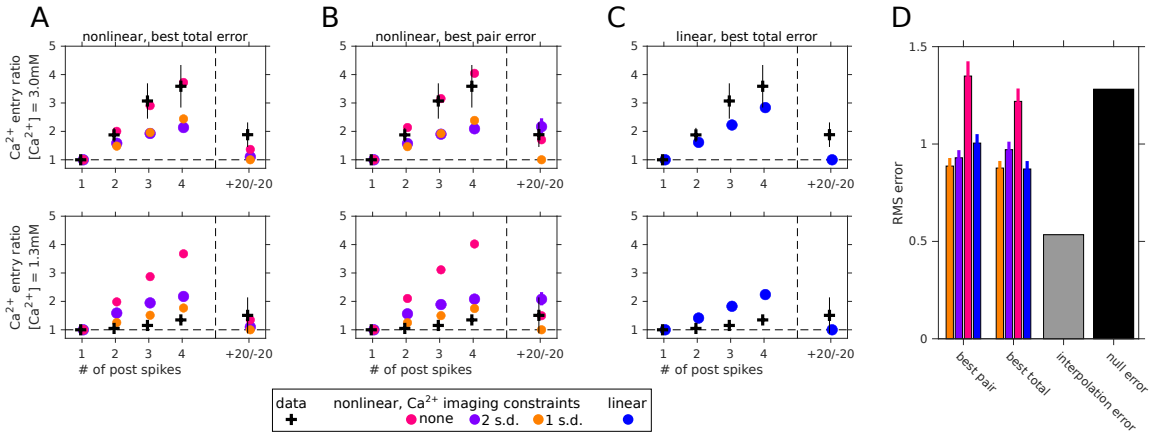

Figure S4: **Using calcium imaging of intracellular transients to constrain models.** For every model variant shown in the paper we plot the total calcium entry ratio as a function of the number of postsynaptic spikes, the relative timing, and the extracellular concentration. Data from protocols with one and two post-synaptic spikes was used to constrain model parameters (see Supplementary Information, Section 3). Protocols measuring calcium entry as a function of timing (Δt =+20/-20 ms, pre-post vs. post-pre, in the same neurons; see **Figure 3** and **Figure S1**) imposed weaker constraints on model parameters, so are shown here despite not being used in the fitting procedure. (**A**) Nonlinear models chosen based on lowest combined error for spike-pair and burst plasticity protocols. (**B**) Nonlinear models chosen based on lowest error for spike-pair plasticity protocols. In panels (**A**) and (**B**) we show results for models fitted subject to constraints imposing varying levels of accuracy relative to the imaging experiments: yellow, 1 standard deviation; purple, 2 standard deviations; red, no constraints from imaging experiments. (**C**) A linear model chosen based on lowest combined error for spike-pair and burst plasticity protocols. (**D**) Root-mean-square error of calcium entry ratios of each model variant averaged over all data points. Similarly to **Figure 8**, gray and black bars indicate estimate of the data variability and the errors of a null model, respectively.

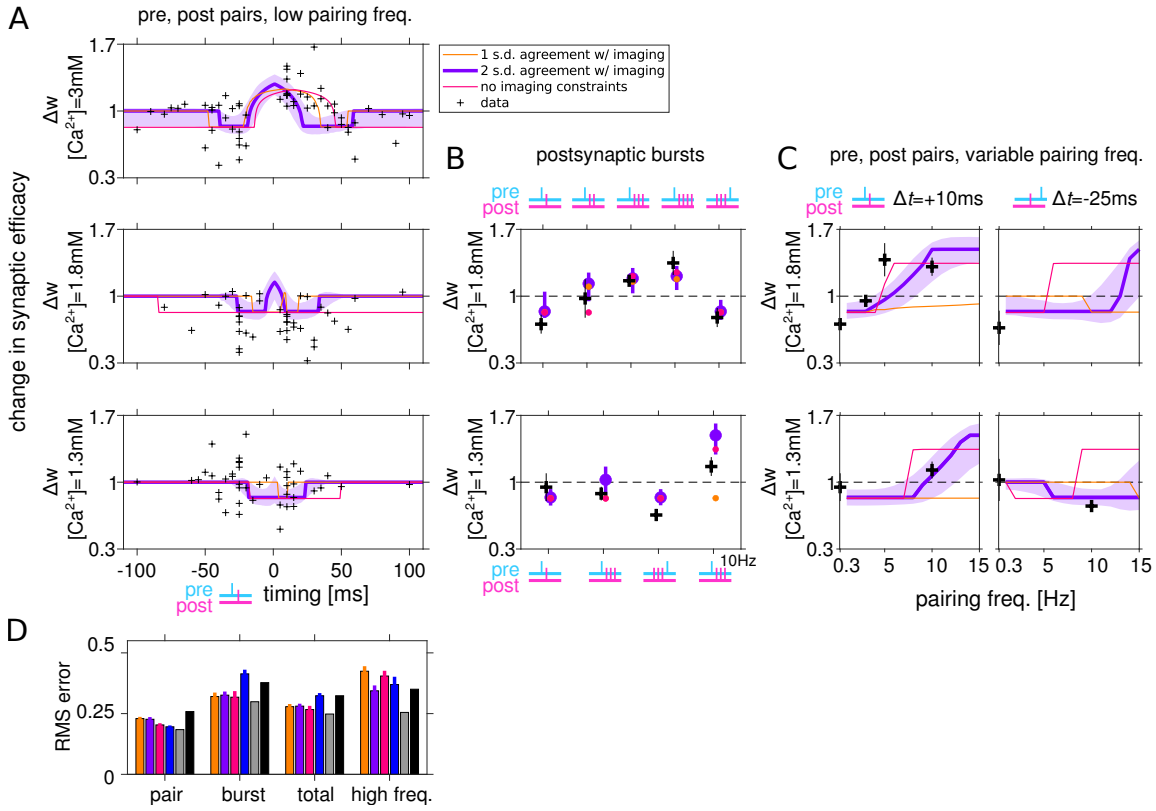

Figure S5: **Constraints on parameters of nonlinear model from imaging experiments improve predictions for high pairing frequency experiments.** Same as **Figure 8**, here we also show results for a nonlinear model where parameters were unconstrained by imaging experiments (red) and using strong/weak constraints based on the imaging experiments (orange/purple). Imposing a weak constraint on parameters using the imaging experiments (2 S.D. of r_2, the ratio of total calcium entry for a two post-synaptic spike stimulus relative to a protocol with a single post-synaptic spike, see Supplementary Information Section 3) leads only to a small increase in the fitting error, and to substantial improvements to the predictions for the high-frequency data not used for fitting or model selection. The imaging experiments thus serve as an important regularization on the fitting procedure. Strong constraints by the imaging experiments (1 S.D. of r_2) lead on the other hand to poor fits and predictions to the plasticity experiments, especially protocols with high pairing-frequencies. (**A**) Model fits to the STDP data at $[Ca^{2+}] = 3, 1.8, 1.3$ mM (lines). Each measured synapse is represented by a black cross. (**B**) Experimental results and model predictions for protocols with post-synaptic burst stimuli. (**C**) Experimental results and model predictions for protocols at variable pairing frequencies and either pre-post or post-pre relative timing. (**D**) Root mean square (RMS) errors when the model predictions are compared to the spike-pair data, the bust data (only at a low pairing frequency of 0.33 Hz), and measurements of plasticity using high-frequency pairing protocols. The total error is the root mean of squared errors computed for the spike-pair and burst stimuli at a low pairing frequency.

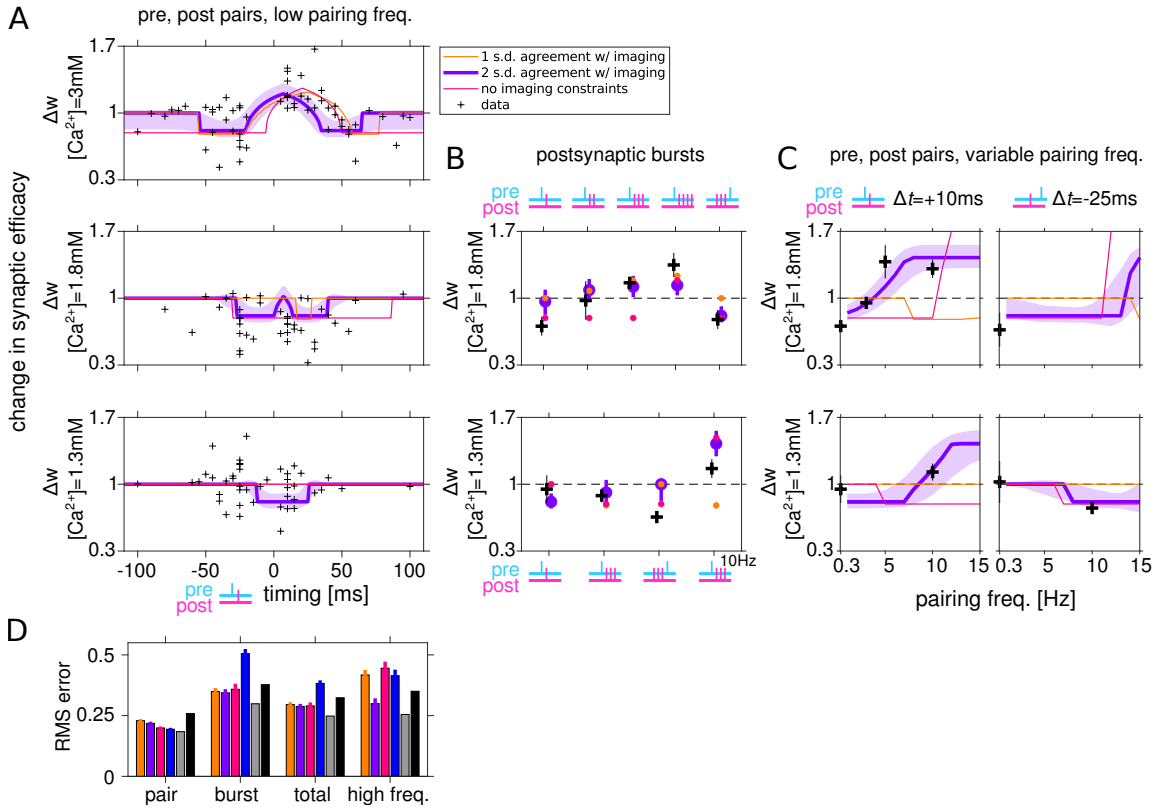

Figure S6: **Nonlinear models fit to spike-pair data alone produce accurate predictions.** Same as **Figure 8**, **Figure S5**, here we show results for parameter sets yielding the lowest fit error to spike-pair data (compared to **Figure 8** where showing results for parameter sets fit to spike-pair data, but selected to have lowest combined spike-pair and burst data error). As expected the prediction error for burst stimuli is increased, but the model is still qualitatively consistent with the entire dataset. In fact, the predictions to the held-out data (high pairing frequency protocols) is better here compared to **Figure 8**, suggesting that our model does not suffer from over-fitting. (**A**) Model fits to the STDP data at $[Ca^{2+}]$ = 3, 1.8, 1.3 mM (lines). Each measured synapse is represented by a black cross. (**B**) Experimental results and model predictions for protocols with post-synaptic burst stimuli. (**C**) Experimental results and model predictions for protocols at variable pairing frequencies and either pre-post or post-pre relative timing. (**D**) Root mean square (RMS) errors when the model predictions are compared to the spike-pair data, the bust data (only at a low pairing frequency of 0.33 Hz), and measurements of plasticity using high-frequency pairing protocols. The total error is the root mean of squared errors computed for the spike-pair and burst stimuli at a low pairing frequency.

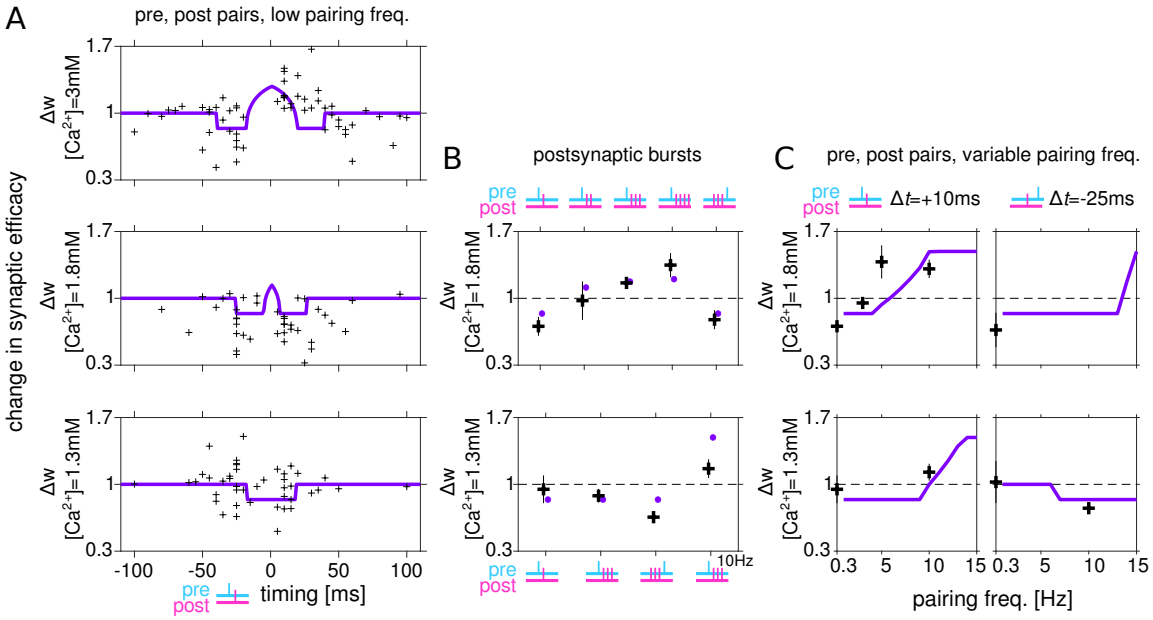

Figure S7: **A nonlinear model without direct post-synaptic contribution to calcium transients produces accurate predictions.** Same as **Figure 8**, here we show results for the same model discussed in the main text, where the post-synaptic contribution is eliminated, i.e., $c(t) = c_{\text{pre}}(t) + c_{\text{NL}}(t)$. Note that here the post-synaptic calcium transient $c$post is used in the evaluation of $c_{\text{NL}}(t)$, but it does not contribute directly to plasticity. The differences in predictions are negligible, with the only appreciable difference being a slight increase in the pairing frequency at which LTD is replaced by LTP at $[Ca^{2+}] = 1.8$ mM, with $\Delta t = +10$ ms. Thus, our model is consistent with experiments showing that repeated post-synaptic stimulation alone, even at high frequencies, does not lead to plasticity.

Supplementary Tables

		Model (imaging constraints)			
Param.	Meaning	nonlinear (none)	nonlinear (2 s.d.)	nonlinear (1 s.d.)	linear (none)
C_{pre}	Pre-synaptic amplitude	0.105	0.135	0.755	0.622
C_{post}	Post-synaptic amplitude	0.127	0.570	0.189	0.340
a_{pre}	Pre-syn. Ca^{2+} exponent	0.594	0.859	0.111	0
a_{post}	Post-syn. Ca^{2+} exponent	1.538	0.499	1.294	0.966
τ_{Ca} (ms)	Ca^{2+} timescale	96.040	18.185	33.961	75.753
D (ms)	Pre-synaptic delay	15.473	0.942	8.668	7.412
θ_p	Potentiation threshold	5.834	3.002	1.173	1.326
γ_d	Depression rate	0.122	1.212	0.388	0.047
γ_p	Potentiation rate	0.944	1.052	1.998	0.332
w_{min}	Minimum synaptic weight	0.829	0.840	0.833	0.781
w_{max}	Maximum synaptic weight	1.411	2.241	1.344	1.394
$\tau_{\text{Ca,NMDA}}$ (ms)	Nonlin. Ca^{2+} timescale	241.521	128.923	162.420	N/A
η (ms^{-1})	Nonlinearity parameter	410.352	414.466	0.00436	N/A
$\varepsilon_{\text{pair}}$	Pre-post pair error	0.203	0.227	0.229	0.196
$\varepsilon_{\text{burst}}$	Post-synaptic burst error	0.317	0.326	0.320	0.414
$\varepsilon_{\text{total}}$	Total low freq. plasticity error (pair & burst)	0.267	0.281	0.279	0.324
$\varepsilon_{\text{freq.}}$	High freq. plasticity error	0.405	0.344	0.424	0.370
$\varepsilon_{\text{imaging}}$	Imaging error	1.219	0.971	0.877	0.872
Corresponding figure		Fig. S5	Fig. 7 Fig. 8 Fig. S2 Fig. S3	Fig. S5	Fig. S2 Fig. S3

Table S1: Parameters and resulting fitting and prediction errors for models chosen based on best combined error for pair and burst plasticity protocols.

		Model (imaging constraints)			
Param.	Meaning	nonlinear (none)	nonlinear (2 s.d.)	nonlinear (1 s.d.)	linear (none)
C_{pre}	Pre-synaptic amplitude	0.0108	0.446	0.558	0.380
C_{post}	Post-synaptic amplitude	0.401	0.141	0.138	0.554
a_{pre}	Pre-syn. Ca^{2+} exponent	2.288	0.681	0.426	0.234
a_{post}	Post-syn. Ca^{2+} exponent	0.643	1.566	1.560	0.319
τ_{Ca} (ms)	Ca^{2+} timescale	70.129	17.946	41.087	191.513
D (ms)	Pre-synaptic delay	20.951	7.169	23.675	6.936
θ_p	Potentiation threshold	5.633	3.816	1.145	1.174
γ_d	Depression rate	1.083	1.133	1.954	0.239
γ_p	Potentiation rate	0.966	0.439	0.660	2
w_{min}	Minimum synaptic weight	0.793	0.816	0.778	0.776
w_{max}	Maximum synaptic weight	2.736	3	3	1.392
$\tau_{\text{Ca,NMDA}}$ (ms)	Nonlin. Ca^{2+} timescale	92.842	149.217	172.758	N/A
η (ms^{-1})	Nonlinearity parameter	342.891	434.382	0.00619	N/A
$\varepsilon_{\text{pair}}$	Pre-post pair error	0.199	0.218	0.229	0.194
$\varepsilon_{\text{burst}}$	Post-synaptic burst error	0.358	0.344	0.349	0.505
$\varepsilon_{\text{total}}$	Total low freq. plasticity error (pair & burst)	0.290	0.288	0.295	0.383
$\varepsilon_{\text{freq.}}$	High freq. plasticity error	0.445	0.299	0.417	0.414
$\varepsilon_{\text{imaging}}$	Imaging error	1.349	0.929	0.887	1.005
Corresponding figure		Fig. S6	Fig. S6	Fig. S6	N/A

Table S2: Parameters and resulting fitting and prediction errors for models chosen based on best error for pair plasticity protocols.

Param.	Meaning	Minimum	Maximum	Comments
C_{pre}	Pre-synaptic amplitude	0.01	1	We set additional constraints so that single neuron (pre/post) transients did not cross θ_d at the highest concentration, $[Ca^{2+}] = 3$ mM.
C_{post}	Post-synaptic amplitude	0.01	1	
a_{pre}	Pre-syn. Ca^{2+} exponent	0	3	
a_{post}	Post-syn. Ca^{2+} exponent	0	3	
τ_{Ca} (ms)	Ca^{2+} timescale	0	100, 250	We used the higher upper bound for the linear model
D (ms)	Pre-synaptic delay	0	40	
θ_p	Potentiation threshold	1 ($= \theta_d$)	10	The depression threshold was fixed to 1, and transient calcium amplitudes were measured relative to it.
γ_d	Depression rate	0.0001	2	We tried increasing the upper bound for γ_d leading in some cases to slightly better fitting errors (see Table 2), but worse predictions.
γ_p	Potentiation rate	0.0001	2	
w_{min}	Minimum synaptic weight	0	1	
w_{max}	Maximum synaptic weight	1	3	
$\tau_{\text{Ca,NMDA}}$ (ms)	Nonlin. Ca^{2+} timescale	80	250	We chose a relatively high lower bound to eliminate interference between the linear and nonlinear calcium transients in the fitting.
η (ms^{-1})	Nonlinearity parameter	0	500	

Table S3: Allowed ranges for parameters in numerical optimization procedure.

Error	Meaning	Data variance estimate	Null Model
$\varepsilon_{\text{pair}}$	Pre-post pair error	0.184	0.258
$\varepsilon_{\text{burst}}$	Post-synaptic burst error	0.299	0.377
$\varepsilon_{\text{total}}$	Total low freq. plasticity error	0.248	0.323
$\varepsilon_{\text{freq.}}$	High freq. plasticity error	0.255	0.350
$\varepsilon_{\text{imaging}}$	Imaging error	0.534	1.282

Table S4: Model fit and prediction errors are compared to (a) an estimate of the data variance (3rd column) and to (b) the error of a null model (4th column). Our estimate of the data's variability is obtained by computing the squared error of every data point relative to the mean of all measurements of the same protocol, averaging over all points within a category of the dataset (pair/burst/high-frequency/imaging), and taking the square-root. For the spike-pair protocols we bin points in terms of Δt and the extracellular calcium so there are at least 2 data points in each bin. The null-model error is computed by assuming no synaptic change under any experimental condition ($\Delta w = 1$). For the imaging experiments, the null model assumes transient calcium amplitude is independent of the extracellular concentration, and the calcium entry is linear in the number of post-synaptic spikes.

References

[1] Michael Graupner and Nicolas Brunel. Calcium-based plasticity model explains sensitivity of synaptic changes to spike pattern, rate, and dendritic location. *Proceedings of the National Academy of Sciences*, 109(10):3991–3996, 2012.

[2] Dimitri M Kullmann, David J Perkei, Toshiya Manabe, and Roger A Nicoll. Ca2+ entry via postsynaptic voltage-sensitive ca2+ channels can transiently potentiate excitatory synaptic transmission in the hippocampus. *Neuron*, 9(6):1175–1183, 1992.

[3] Robert C Malenka and Roger A Nicoll. Nmda-receptor-dependent synaptic plasticity: multiple forms and mechanisms. *Trends in neurosciences*, 16(12):521–527, 1993.